

## METHODS FOR MEASURING THE POWER LINEARITY OF MICROWAVE DETECTORS FOR RADIOMETRIC APPLICATIONS\*

V. S. Reinhardt, Y. C. Shih, P. A. Toth, S. C. Reynolds, and A. L. Berman  
Hughes Space & Communications Company, Los Angeles, California

### Abstract

A microwave radiometer relies on the power linearity of its microwave receivers to accurately measure the temperature of remote microwave noise sources. This paper considers linearity issues in the design and characterization of such receivers. Analysis is presented relating the radiometer temperature interpolation error to a second order power nonlinearity coefficient for the receiver. Formulas are also developed specifying the temperature error in terms of individual receiver component parameters. It is shown that the key parameter for the RF detector in the receiver is  $A_4$ , a fourth order RF distortion coefficient, and the key parameter for the RF amplifiers in the receiver is  $IP_3$ , the third order intercept. This paper also discusses experimental methods for measuring the power linearity of RF detectors to the levels required for radiometric applications. Three methods are discussed: the two-tone method, the amplitude modulation method, and the constant ratio method. The theory of determining the coefficients that characterize the nonlinearity of the detector from experimental data is presented. Experimental results are presented showing that the two-tone method and the constant ratio method agree to within experimental error. The sensitivity for measuring nonlinearities and the difficulties encountered in implementing each of these methods are also discussed.

### Introduction

A microwave radiometer relies on the power linearity of its microwave receivers to accurately measure the temperature of remote microwave noise sources<sup>1,2,3,4,5,6,9</sup>. Figure 1 shows how a typical radiometer measures a remote scene temperature  $T$  by periodically scanning an antenna feed and receiver between a cold load at temperature  $T_c$ , a hot load at temperature  $T_h$ , and the remote scene while recording the noise power at the output of the receiver. A typical radiometric receiver consists of a low noise amplifier (LNA) or mixer-local oscillator (LO) which establishes a receiver noise figure  $F$ . A bandpass filter establishes a noise or convolution bandwidth  $B$ , and an RF detector and video amplifier provide a video voltage output  $V$  that is assumed to vary linearly with  $P$  the effective noise power at the antenna input given by

$$P = k B [T + (F - 1)T_o] \quad (1)$$

\* Work performed under NASA GSFC contract NAS5-32018, TRMM Microwave Imager.

where  $k$  is Boltzman's constant and  $T_0$  is 290 K. By measuring  $V$  when the antenna feed is pointed to  $T_c$ ,  $T_h$ , and  $T$ , one can determine  $\hat{T}$  an estimate of  $T$  using the linear interpolation formula

$$\hat{T} - T_c = \frac{T_h - T_c}{V_h - V_c} (V - V_c) \quad (2)$$

Typically, the radiometer must interpolate  $T$  to a fraction of a degree K out of a system noise temperature of 1000 K or more. Thus, the power linearity of the receiver is a critical issue in determining the accuracy of this interpolation. This paper will consider such power linearity issues in the design and characterization of radiometric receivers. The first section will develop formulas for characterizing the nonlinear temperature error in terms of the RF properties of the receiver and individual receiver components. The next section will deal with experimental methods for measuring the power linearity of RF detectors used in radiometric receivers.

### **Power Linearity Considerations in the Design of a Radiometric Receiver**

In this section, a formula for the temperature interpolation error due to a second order receiver power nonlinearity and detailed formulas relating the nonlinear temperature error to RF nonlinearity parameters of individual receiver components will be developed.

#### **Temperature Error Due to 2nd Order Power Nonlinearity**

Let us assume the receiver has a small second order power nonlinearity given by

$$V \propto P - C P^2 \quad (3)$$

Using (1), (2), and (3), one can show that the worst case interpolation temperature error  $\delta T_L = T - \hat{T}$  is given by

$$\frac{\delta T_L}{T_h - T_c} = \frac{C}{4} (P_h - P_c) \quad (4)$$

where it is assumed that  $|CP| \ll 1$ . Using typical parameters for a spaceborne radiometer, (4) can be approximated by

$$\frac{\delta T_L}{T_0} \cong \frac{C}{4F} P_h = \frac{1}{4F} \frac{\delta P_h}{P_h} \quad [T_c \cong 0 \text{ K}, T_h \cong T_0] \quad (5)$$

where  $\delta P = CP^2$ . From (5) using typical values of  $\delta T_L = 0.3$  K and  $F = 4$  dB, one can see that the maximum allowable power nonlinearity for a spaceborne radiometric receiver is  $\delta P_h / P_h$  is -20 dB.

### Temperature Error Due to RF Component Nonlinearities

Let us now utilize the model of the radiometric receiver shown in Figure 2 to develop formulas for relating  $\delta T_L$  to individual component nonlinearity parameters. This model first contains an RF amplifier, representing a composite of all RF amplifiers and mixers, surrounded by two bandpass filters with time domain response functions and noise bandwidths  $h_1(t)$ ,  $B_1$  and  $h_2(t)$ ,  $B_2$ . Next are an RF detector with a power sensitivity  $K_D$  and a video amplifier. In the following subsections, we will show how the non-square law behavior of the detector or the receiver as a whole and the third order intermodulation distortion of the RF amplifier both contribute to the coefficient  $C$ .

**Power Nonlinearity to Due Non-Square Law RF Behavior.** A radiometric receiver and the RF detector and video amplifier in that receiver ideally act as perfect square law detectors of their respective RF inputs. Using Wiener-Volterra<sup>6</sup> analysis and assuming that nonlinear device bandwidths are much larger than that of the linear filters in the receiver, one can show that the receiver video output  $V$  can be written in terms of the bandlimited RF voltage  $V_r$  (see Figure 2) as

$$V = A_2 \langle V_r^2 \rangle + A_4 \langle V_r^4 \rangle + \dots \quad (6)$$

where  $\langle X \rangle$  represents the expectation value of  $X$  over an infinite time or ensemble average and where it is assumed that  $\langle V_r^{2n+1} \rangle = 0$ .

For a radiometric receiver,  $V_r$  is bandlimited thermal noise which can be represented by

$$V_r(t) = \int h(t-t') f(t') dt' \quad (7)$$

where (a)

$$h(t-t'') = \int h_2(t-t') h_1(t'-t'') dt' \quad (8)$$

represents the composite of filter 1 and 2 with a total noise bandwidth of

$$B = (1/2) \int h(t)^2 dt \quad (9)$$

(b) it is assumed that both filters are lossless and the RF amplifier has unity gain, and  
(c)  $f(t)$  is a random Langevin function<sup>7,8</sup> whose 2nd and 4th order autocorrelation functions are

$$\langle f(t) f(t') \rangle = \frac{N_0}{2} \delta(t-t') \quad (10)$$

$$\langle f(t_1)f(t_2)f(t_3)f(t_4) \rangle = (N_0/2)^2 [\delta(t_1-t_2)\delta(t_3-t_4) + \delta(t_1-t_3)\delta(t_2-t_4) + \delta(t_1-t_4)\delta(t_2-t_3)] \quad (11)$$

with

$$N_0 = k T_s = k [T + (F-1)T_0] \quad (12)$$

Noting that  $P = \langle V_r^2 \rangle$  and substituting (7) into (6), one obtains to fourth order

$$V = A_2 P + A_4 \int h(t-t_1) \dots h(t-t_4) \langle f(t_1)f(t_2)f(t_3)f(t_4) \rangle dt_1 \dots dt_4 \quad (13)$$

Finally using (1), (9), (11), and (12), one can show that (13) becomes

$$V = A_2 P + 3 A_4 (N_0 B)^2 = A_2 P + 3 A_4 P^2 \quad (14)$$

Thus, the nonlinearity coefficient is

$$C = -3 \frac{A_4}{A_2} \quad [\text{Bandlimited Noise Input}] \quad (15)$$

Note that there is a different relationship for a CW input

$$C = -\frac{3 A_4}{2 A_2} \quad [\text{CW Input}] \quad (16)$$

**Nonlinearity Figure of Merit for RF Detector.** Before proceeding to discuss the RF amplifier, let us utilize (15) to define a figure of merit for the acceptability of an RF detector in a particular radiometric application. From (5) and (15), one can write

$$P_{dh} = \frac{4F}{3} \left| \frac{A_2}{A_4} \right| \frac{\delta T_{Ld}}{T_0} \quad (17)$$

where  $P_{dh}$  is the power into the detector at which  $|\delta T_L|$  reaches the allocated value  $\delta T_{Ld}$ . One can show that the lowest power that can be input to the detector while meeting radiometer noise equivalent  $\delta T$  (NE $\delta T$ ) requirements can be written as<sup>4</sup>

$$P_{dm} = \frac{V_n T_{sm}}{K_d \delta T_V} \quad (18)$$

where  $V_n$  is the equivalent input voltage noise of the video amplifier,  $\delta T_V$  is the allocated contribution of the video amplifier to the total  $NE\delta T$ ,  $K_d$  is the detector diode sensitivity, and  $T_{sm}$  is the system noise temperature at the minimum scene temperature. Using (17) and (18), one can define a figure of merit for the detector as

$$M_d = \frac{P_{dh}}{P_{dm}} = \frac{4F}{3} \left| \frac{K_d A_2}{V_n A_4} \right| \frac{\delta T_{Ld}}{T_o} \frac{\delta T_V}{T_{sm}} \quad (19)$$

which gives the detector's allowable operating range ( $M_d > 1$  for a suitable detector). Thus, the suitability of a detector diode for radiometric applications depends both on its linearity given by  $A_4/A_2$  and its sensitivity given by  $K_d$  (as well as the noise of the video amplifier given by  $V_n$ ).

**Effects of RF Amplifier Nonlinearity.** Finally, let us consider the effect of RF amplifier distortion on the coefficient  $C$ . Again, Figure 2 defines the components and variables. The amplifier is modeled by

$$V_o = V_i + \sum_{n=2} a_n V_i^n \quad (20)$$

Using (20), one can write the voltage into the RF detector as

$$V_r(t) = \int h(t-t') f(t') dt' + a_3 \int h_2(t-t') \left[ \int h_1(t'-t'') f(t'') dt'' \right]^3 dt' \quad (21)$$

where we have assumed that Filters 1 and 2 are narrow enough to filter out the  $a_2$  term, which generates only DC and second harmonic components. Utilizing the first term in (6) and (1), (10), (11), (12), and (21), it can be shown that

$$V \cong A_2 \langle V_r^2 \rangle = A_2 [P + 6 a_3 (B_1/B) P^2] \quad (22)$$

where  $B_1$  is defined similarly to (9) with  $h_1(t)$  substituted for  $h(t)$ . Since  $B_1 \geq B$ ,  $C$  is minimized when  $B_1 \cong B$ . This is accomplished by using Filter 1 to set the noise bandwidth  $B$  and making Filter 2 just narrow enough to filter out the second harmonic distortion of the RF amplifier. Comparing (22) to (3), we finally obtain

$$C = -6 a_3 (B_1/B) \quad (23)$$

One can show that  $IP_3$  the RF amplifier's the third order intercept for a coherent CW input is equal to

$$IP_3 = \frac{2}{|a_3|} \quad (24)$$

by expanding (2) for a coherent input and setting the asymptotic third order intermodulation ratio to one. Using (24) in (23) then yields

$$|C| = \frac{12 B_1}{IP_3 B} \quad (25)$$

Thus, the contribution to C from the RF amplifier can be determined by measuring  $IP_3$ .

### Methods for Measuring the Linearity of RF Detectors

In the following subsections we will describe three methods for measuring  $A_4/A_2$  in RF detectors to the levels required for radiometric applications.

#### The Two-Tone Method

The two-tone method for measuring diode nonlinearity is shown in Figure 3. Here, two equal power RF signals with frequencies at  $f_0$  and  $f_0+f_m$  are added to generate a modulated RF signal  $V_{RF}$  which is applied to the detector under test. The video output, which consists of harmonics of amplitude  $B_k$  at frequencies  $kf_m$  ( $k=0,1,2,\dots$ ), is then monitored on a low frequency spectrum analyzer. These video harmonics can be utilized to determine  $A_4$  and higher order nonlinearity coefficients describing the RF detector output as follows.

Let the RF input to the detector be given by

$$V_r = P_0^{0.5} [\text{Cos}(\omega_0 t) + \text{Cos}((\omega_m + \omega_0)t)] \quad (26)$$

Utilizing (26) in (6) and assuming that a low pass filter eliminates RF components from V, one can show that<sup>4</sup>

$$V = \sum_k b_k \text{Cos}(k \omega_m t) \quad (27)$$

where

$$b_k = \sum_{n=k}^{\infty} P_0^n A_{2n} b_{kn} \quad (28)$$

and the  $b_{kn}$  are given by the expansion

$$[\text{Cos}(\omega_o t) + \text{Cos}((\omega_m + \omega_o)t)]^{2n} = \sum_{k=0}^n b_{kn} \text{Cos}(k \omega_m t) \quad (29)$$

Table 1 lists the first few  $b_{kn}$  coefficients. From the table, we obtain

$$\frac{b_2}{b_1} = \frac{3}{4} \frac{A_4}{A_2} P_o \quad \left[ \frac{A_4}{A_2} P_o \ll 1 \right] \quad (30)$$

Thus  $(A_4/A_2)$  can be straightforwardly determined from the ratio of the amplitudes of the first and second harmonics of the video output.

**Table 1. Two-Tone Coefficients  $b_{kn}$**

	<b>k = 0</b>	<b>k = 1</b>	<b>k = 2</b>	<b>k = 3</b>	<b>k = 4</b>
<b>n = 1</b>	1	1	0	0	0
<b>n = 2</b>	9/4	3	3/4	0	0
<b>n = 3</b>	25/4	75/8	15/8	5/8	0
<b>n = 4</b>	1225/64	245/8	245/8	35/8	35/64

### The Amplitude Modulation Method

When two RF frequency sources are not available, one can utilize the amplitude modulation technique shown in Figure 2 to measure diode power linearity. Here a linear modulator, an audio oscillator, and a single RF frequency source generates the modulated RF voltage. Again, the  $b_k$  are measured with a spectrum analyzer, and  $b_k$  is related to coefficients  $b_{kn}$  by (28). For this method, however, the  $b_{kn}$  are given by<sup>4</sup> Table 2. The primary limitation of this method is the linearity of the modulator. The sensitivity in measuring  $B_k$  for both the two-tone and amplitude modulation methods is limited by the presence of intermodulation (IM) products in the RF signal impinging on the detector.

**Table 2. Amplitude Modulation Coefficients  $b_{kn}$**

	<b>k = 1</b>	<b>k = 2</b>	<b>k = 3</b>	<b>k = 4</b>
<b>n = 1</b>	2	1/2	0	0
<b>n = 2</b>	7	7/2	1	1/8

### Constant Ratio Method

The constant ratio method is shown in Figure 5. Here one utilizes an attenuator A to set an RF power level from a single LO to a value  $P_k$ . A second attenuator B is then used to change  $P_k$  by an unspecified but constant ratio Q while a digital voltmeter measures the detector video output values  $Y(P_k)$  and  $Y(QP_k)$ . For a linear power detector, we note that

$$D_k = \frac{Y_1(P_k)}{Y_2(QP_k)} \quad (31)$$

is a constant  $Q^{-1}$ . Thus, changes in  $D_k$  when varying  $P_k$  reflect the power nonlinearity level of the detector. One can show that<sup>4</sup>

$$M = \frac{D_1}{D_2} - 1 \cong \frac{3}{2} \frac{A_4}{A_2} (1-Q)(P_1 - P_2) \quad (32)$$

For  $Q=0.5$  and  $P_2=0.5P_1$ , one can show that the measurement error is minimized<sup>4</sup> and that

$$M \cong \frac{3}{8} \frac{A_4}{A_2} P_1 \quad [Q=0.5, P_2=0.5P_1] \quad (33)$$

## Experimental Comparison of Two-Tone and Constant Ratio Methods

To verify the accuracy of the two-tone and constant ratio methods, both were implemented on a detector diode at 6 GHz. For the two-tone measurement, one has to be careful about the generation of intermodulation (IM) products through direct coupling of the RF sources, since these IMs can generate spurious  $b_k$  signals at the detector output, limiting the sensitivity of the  $b_2/b_1$  measurement. In the experimental setup, these IMs were reduced by placing isolators and attenuators after each of the RF sources. A worst case IM level due to source coupling of -79 dB was achieved.

Figure 6 plots the measured  $b_k$  magnitudes as a function of the RF power into the detector along with theoretical 2k dB/dB curves (dotted lines). Observing this 2k dB/dB behavior (leading terms in (28)) is an important indicator that there is no contamination of the data by IMs from the RF sources. The slight deviation of the measured values from 2k dB/dB behavior at the high RF power is due to the higher order terms in (28). These deviations are useful in obtaining the signs of the  $b_k$  from the measured magnitude data so that a polynomial characterizing the detector video voltage as a function of input RF power can be generated.

The limiting sensitivity factor in the  $b_2/b_1$  measurement was the -79 dB source IM level. (The spectrum analyzer noise level of -135 dBm did not limit the measurement.) (15) and (30) can be rewritten as

$$\frac{\delta P}{P_0} = CP_0 = 4 \frac{b_2}{b_1} \quad [\text{Bandlimited White Noise}] \quad (34)$$

so the the two-tone measurement sensitivity achieved for  $\delta P/P_0$  was -73 dB.

The constant ratio method was more difficult to implement than the two-tone method. The accuracy of the 6 GHz measurement was limited by drifts in the power ratio Q generated by Attenuator B, the RF amplitude of the signal generator, and the DC video voltage measurements. Measurement had to be made quickly to minimize the effects of these drifts. To minimize coupling between the attenuators, it was also found necessary to utilize many isolators around Attenuators A and B. The standard error for the average M measurement was  $4.4 \times 10^{-4}$  or -34 dB. Rewriting (15) and (33) yields

$$\frac{\delta P}{P_0} = CP_0 = 8M \quad [\text{Bandlimited White Noise}] \quad (35)$$

so the constant ratio measurement sensitivity achieved for  $\delta P/P_0$  was -25 dB.

Figure 7 shows a comparison of the two-tone and constant ratio results for the 6 GHz tunnel diode. The measurement data has been converted to an equivalent temperature nonlinearity error using (5) and (15) assuming a noise figure F of 4 dB. Note the excellent agreement between the two methods.

## Conclusions

**Table 3. Summary of Important Formulas [ $T_c \cong 0$  K,  $T_h \cong T_0$ ]**

Item	Comment	Equation	Reference Equations
1	Detector/Video Amp $\delta T_L$	$\frac{\delta T_{Ld}}{T_0} \cong \frac{3}{4F} \frac{A_4}{A_2} P_h$	(5),(15)
2	RF Amp $\delta T_L$	$\frac{\delta T_{La}}{T_0} \cong \frac{3}{F} \frac{B_1}{B} \frac{P_h}{IP_3}$	(5),(25)
3	$A_4/A_2$ From Two Tone Method	$\frac{A_4}{A_2} = \frac{4}{3P_0} \frac{b_2}{b_1}$	(30)
4	Detector Figure of Merit (Must be > 1)	$M_d = \frac{4F}{3} \left  \frac{K_d A_2}{V_n A_4} \right  \frac{\delta T_{Ld}}{T_0} \frac{\delta T_V}{T_{sm}}$	(19)

It has been shown that  $\delta T_L$ , the radiometric temperature error due to receiver power nonlinearities, can be determined from the second order power nonlinearity of the receiver output. It has been further shown that this power nonlinearity can be related to the fourth order RF coefficient of the detector and video amplifier in the

receiver and the third order intercept of the final RF amplifier in the receiver. Table 3 summarizes some important formulas developed in this paper. The second column describes the formula and the final column gives the paper equations used to generate the formula shown. Items 1 and 2 give the  $\delta T_L$  contributions for the detector/Video Amp and the RF amplifier in terms of radiometer and component parameters. Item 3 gives the value of  $A_4/A_2$  obtained from the two-tone method for use in Item 1. Finally, Item 4 gives the formula for  $M_D$ , the detector figure of merit.  $M_D$  must be greater than one for a suitable detector.

Table 4 summarizes the achieved or projected obtained with the three methods for measuring detector power nonlinearities. Two of the methods, the two-tone method and constant ratio method, have been experimentally demonstrated to agree within experimental error. The two-tone method has been found to be very sensitive and is well suited for production level detector linearity measurements.

**Table 4. Nonlinearity Sensitivities of Detector Measurement Methods.**

Method	$\delta P/P_O$ Sensitivity	$\delta T_L$ Sensitivity (F = 4 dB)	Comments
Two-Tone	-73 dB	$1.5 \times 10^{-6}$ K	Measured
Amplitude Modulation	-32 dB	0.02 K	Based on -40 dB Modulator Linearity
Constant Ratio	-25 dB	0.1 K	Measured

### Acknowledgments

The Authors would like to acknowledge helpful comments and criticisms from B. Walsh, T. Shishido, M. Hersman, and E. Lobl of Hughes Space and Communications Company. The authors would also like to especially acknowledge the help of R. Sorace of Hughes Space and Communications Company for his work in checking the accuracy of the equations presented and for his suggestions on how to better organize this paper.

### References

- <sup>1</sup> R. M. Price, "Radiometer Fundamentals" in Methods of Experimental Physics, ed. M. L. Meeks, V. 12, Part B, Academic Press, 1976.
- <sup>2</sup> G. Evans and C. W. McLeash, RF Radiometer Handbook, Artech House, 1977.
- <sup>3</sup> J. J. Stacey, Spaceborne Microwave Imagers, JPL Publication 86-37, November 1, 1986.

- 4 V. S. Reinhardt, Y. C. Shih, P. A. Toth, and S. C. Reynolds, "Detector Power Linearity Requirements And Verification Techniques For TMI Direct Detection Receivers," TRMM Microwave Imager Report NASA GSFC NAS5-32018, February, 1993.
- 5 M. S. Hersman and G. A. Poe, "Sensitivity of the Total Power Radiometer with Periodic Absolute Calibration," IEEE Trans. Microwave Theory and Techniques, MTT-29, No. 1, pp. 33-40, January 1981.
- 6 J. J. Bussgang, et. al., "Analysis of Nonlinear Systems with Multiple Inputs," Proceedings of the IEEE, V. 62, No. 8, pp. 1088-1119, August 1974.
- 7 A. Van Der Ziel, Noise, Sources, Characterization, Measurement, Pentice-Hall, 1970.
- 8 N. Wax, Noise and Stochastic Processes, Dover, 1954.
- 9 V. S. Reinhardt, Y. C. Shih, P. A. Toth, S. C. Reynolds, and A. L. Berman, "Methods for Measuring the Power Linearity of Microwave Detectors for Radiometric Applications," 1994 IEEE MTT-S International Microwave Symposium Digest, San Diego, May 23-27, 1994.

Figures

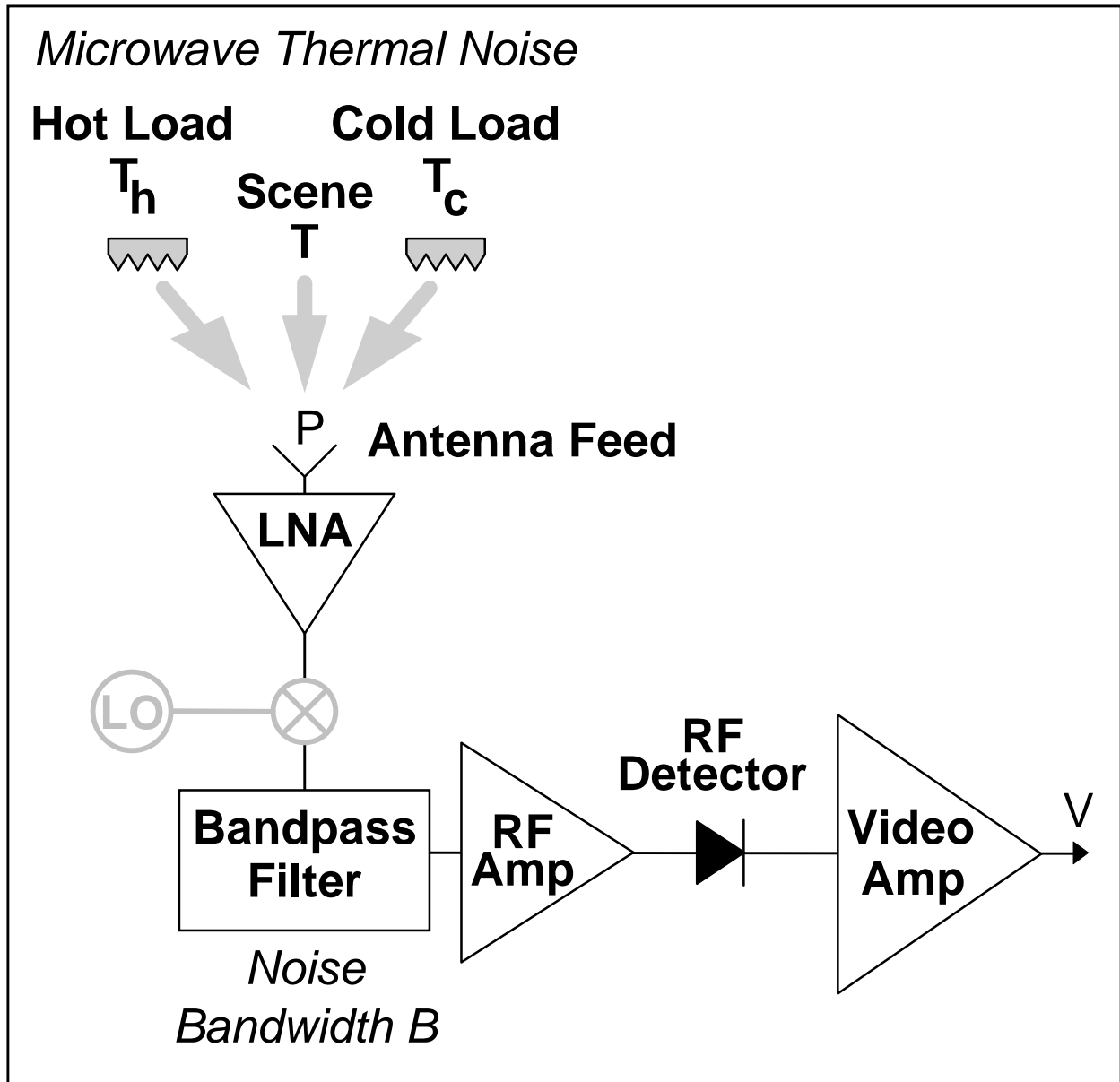


Figure 1. Typical Microwave Radiometer

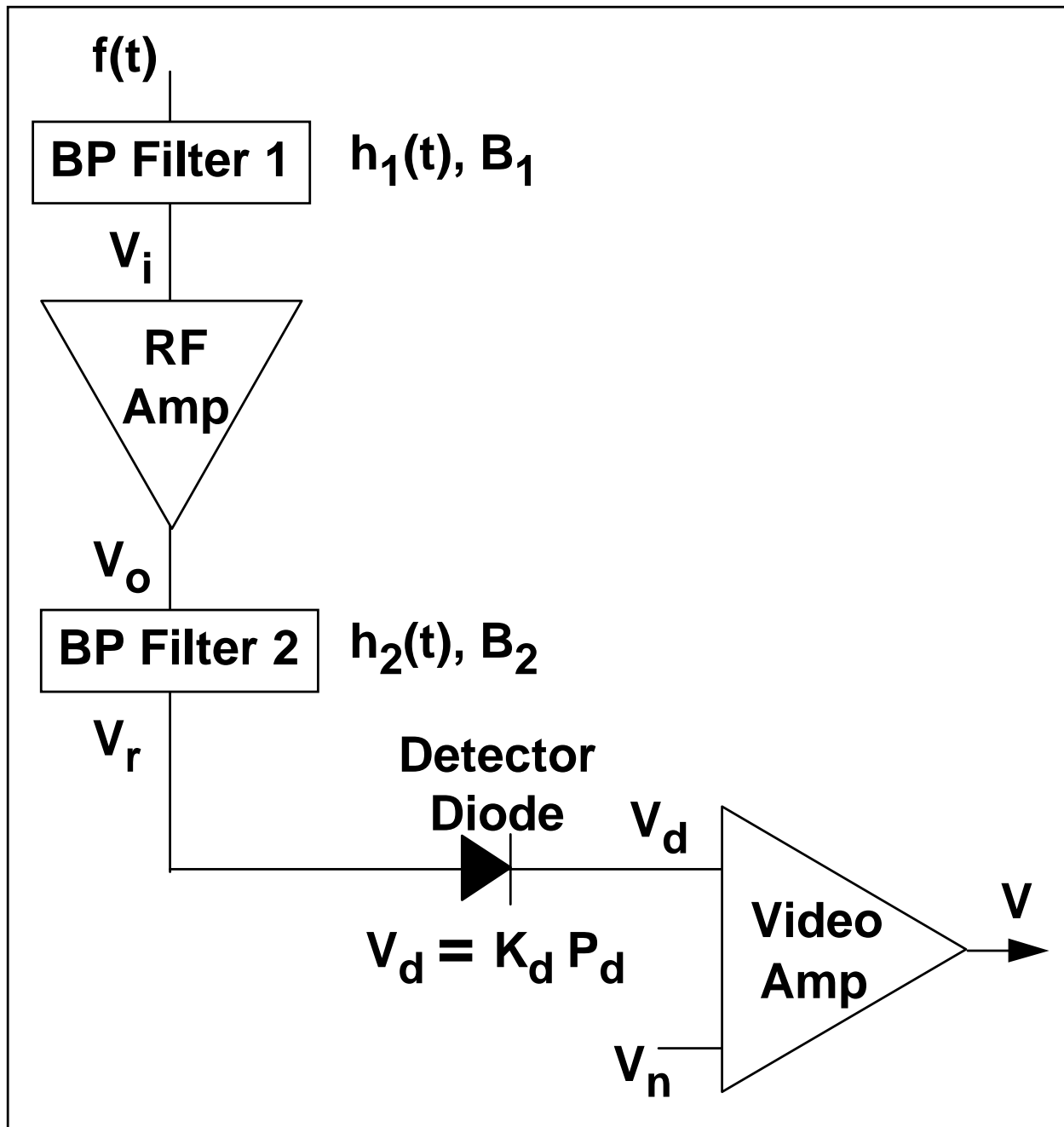


Figure 2. Model of Radiometric Receiver

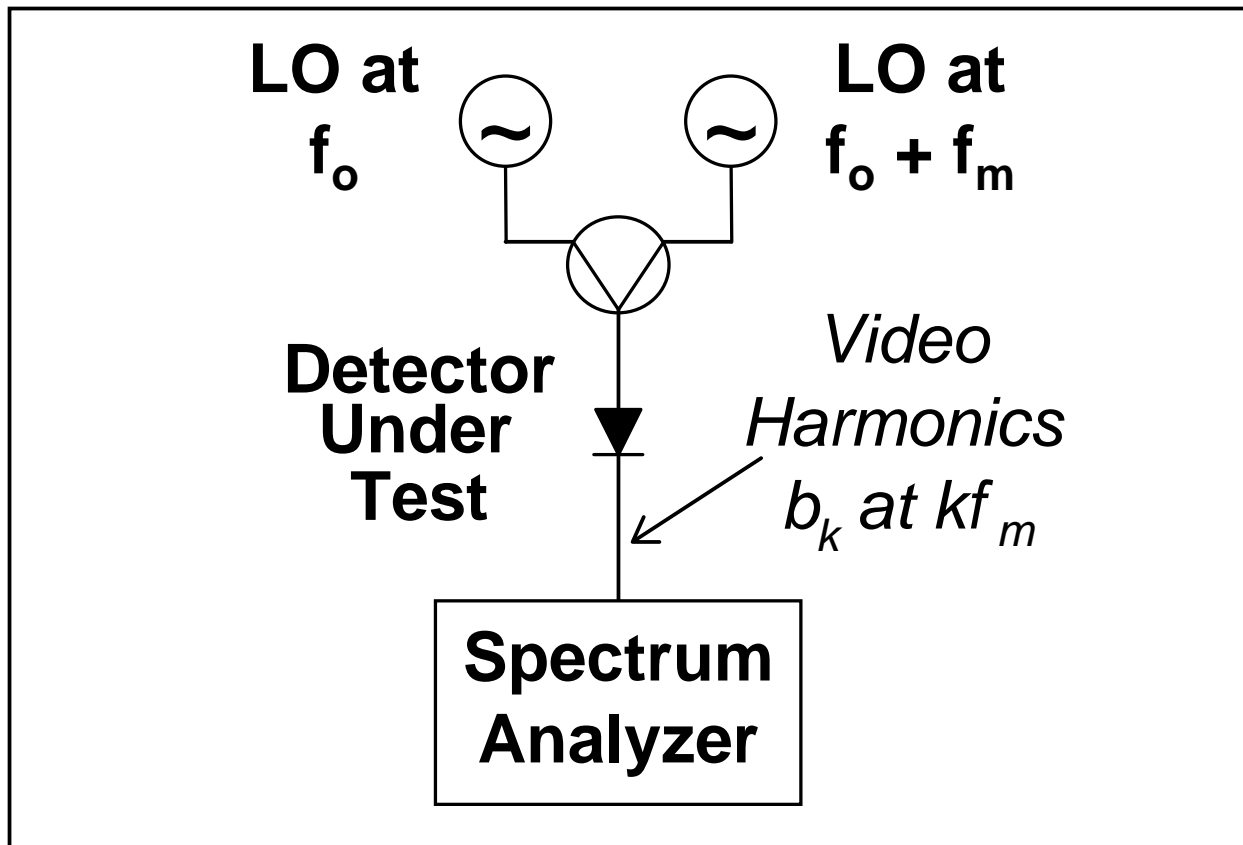


Figure 3. The two-tone method for measuring detector nonlinearity.

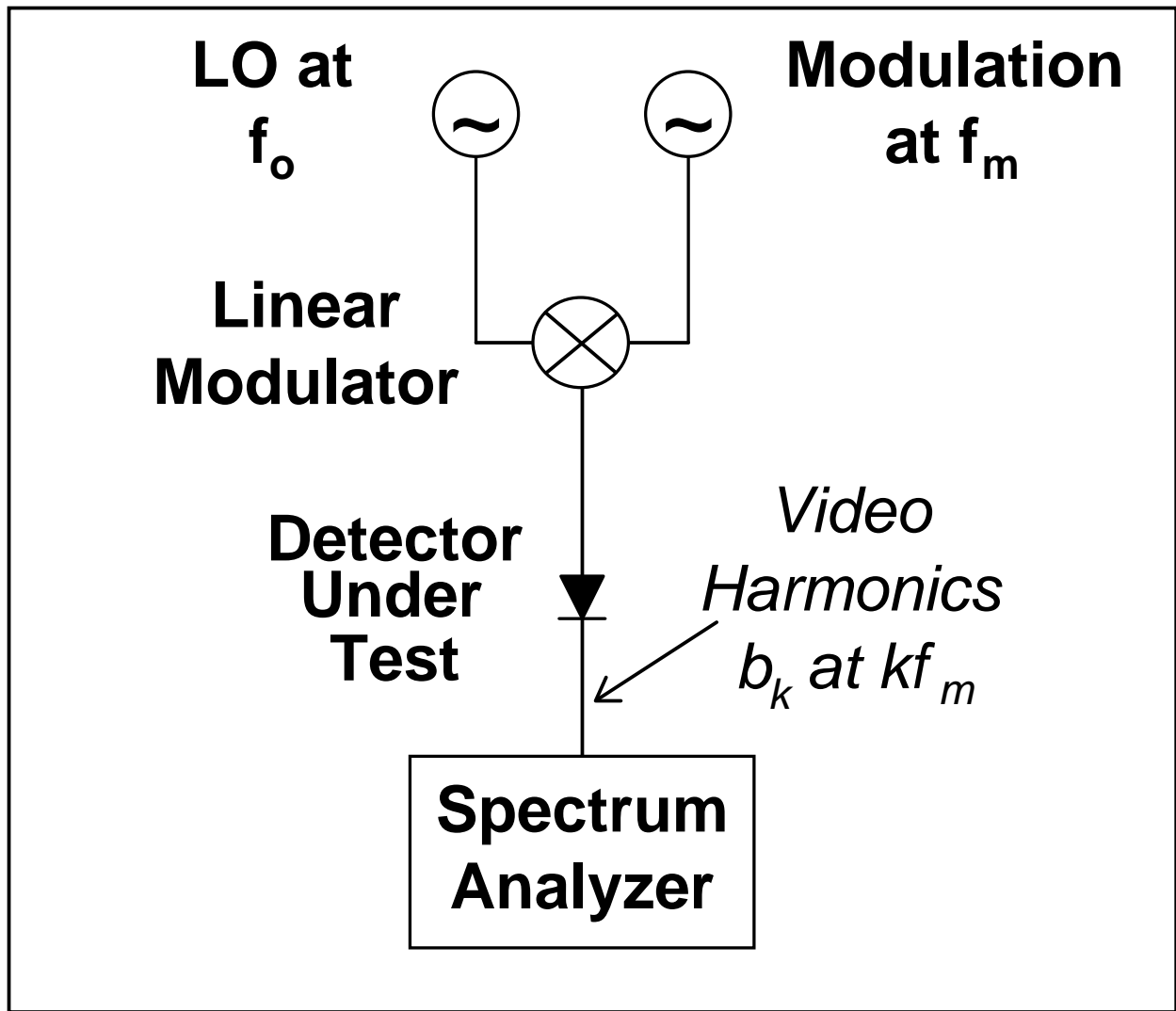


Figure 4. The amplitude modulation method for measuring detector nonlinearity.

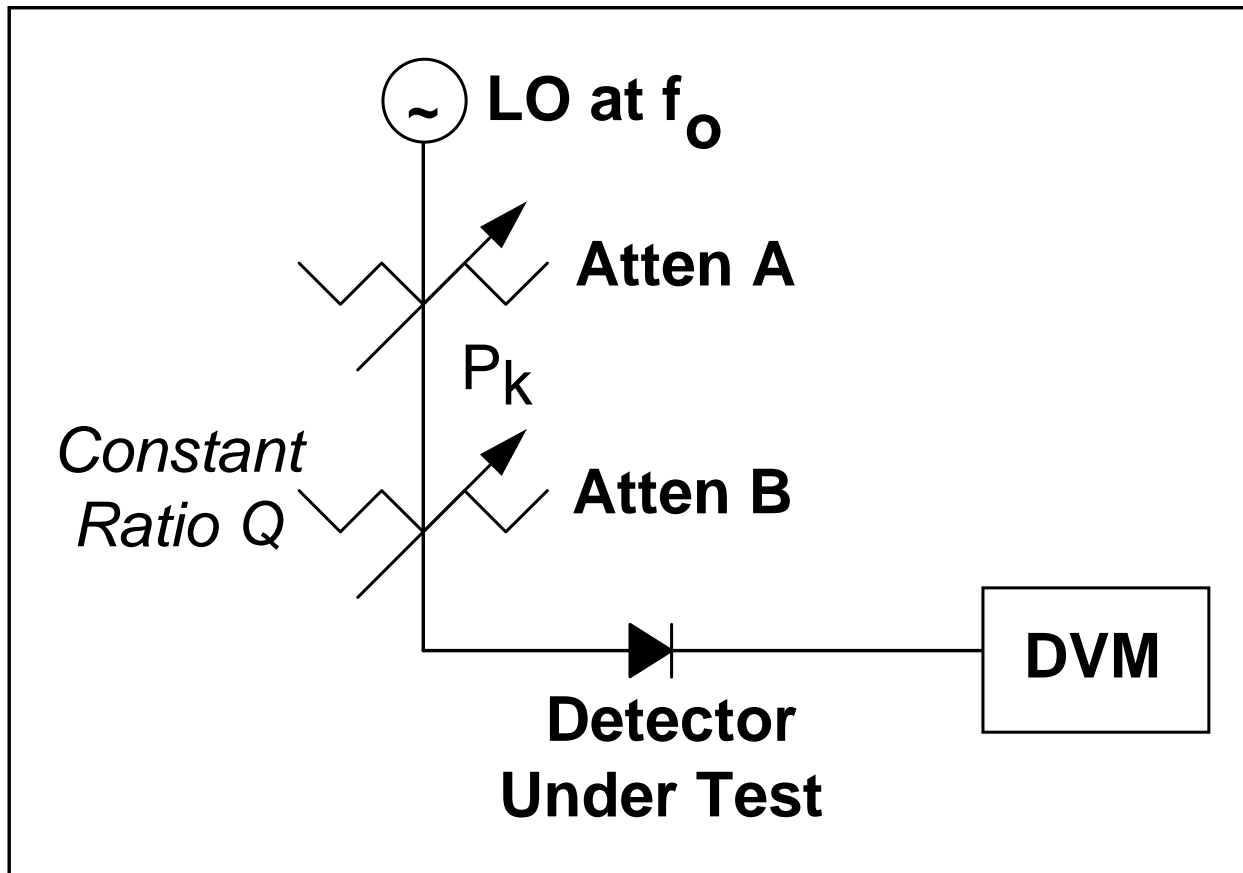


Figure 5. The constant ratio method for measuring detector nonlinearity.

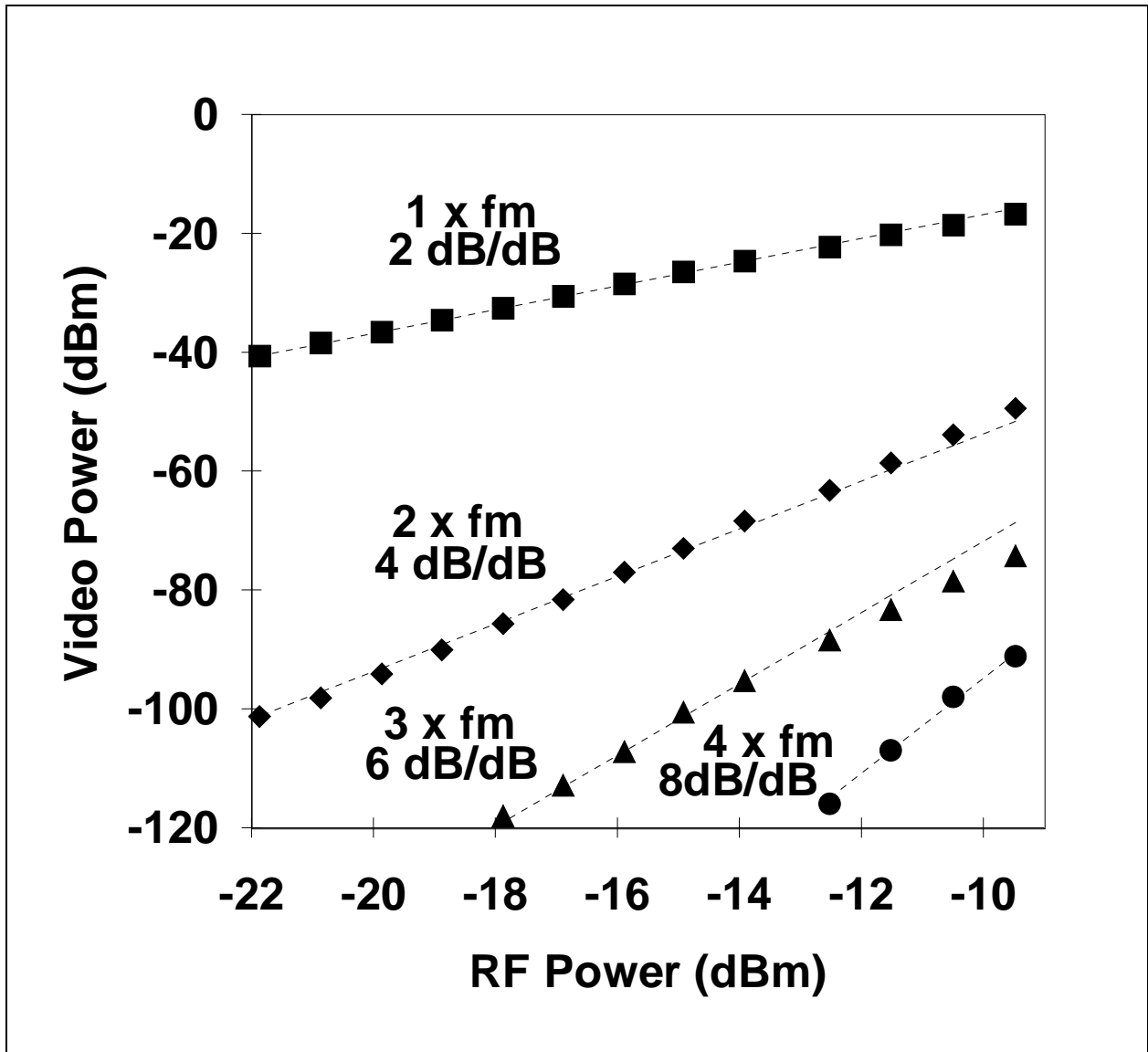


Figure 6. Video two-tone spectrum of tunnel diode at 6 GHz.

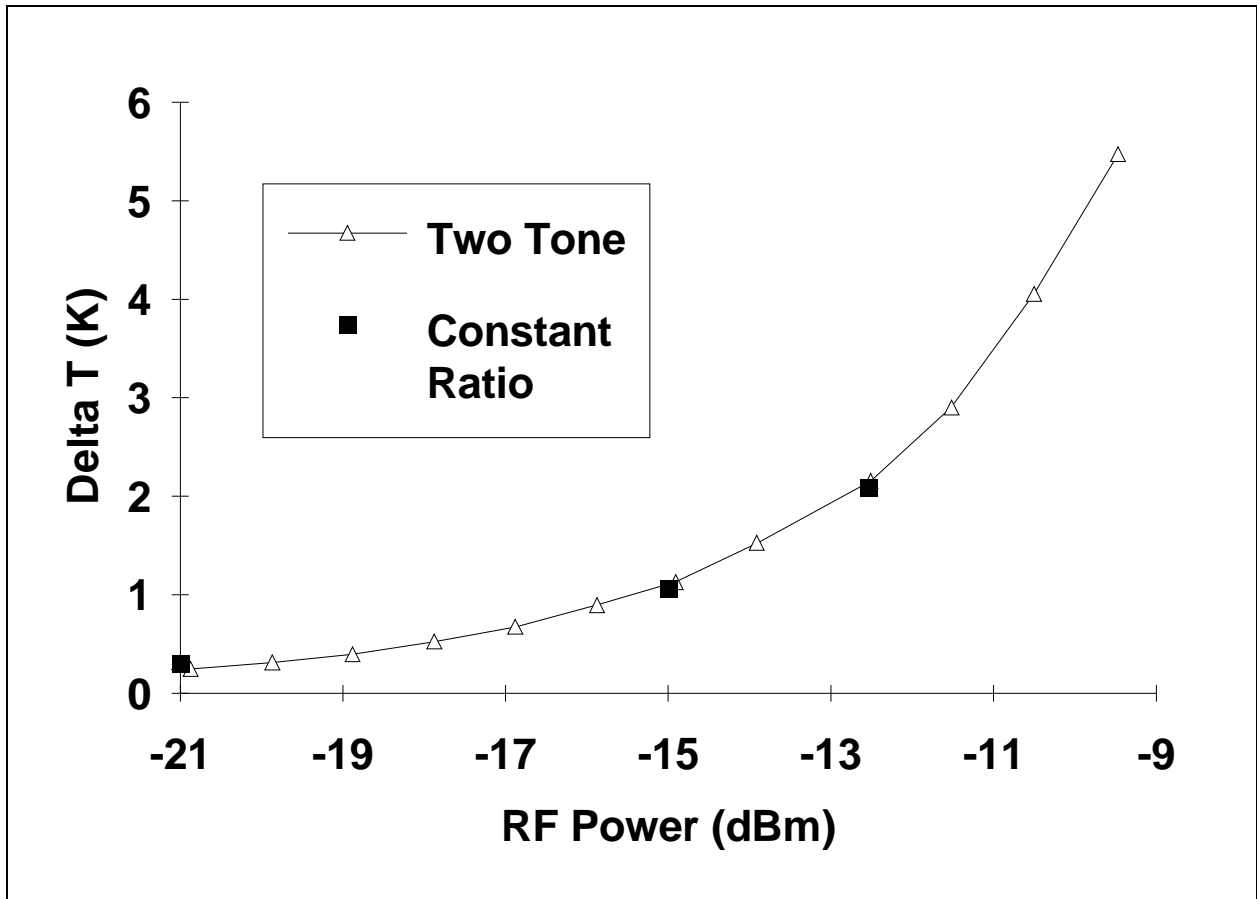


Figure 7. Comparison of two-tone and constant ratio results at 6 GHz.